8

Sources of pairing in nuclei

In general the two-body pairing force is parametrized in terms of: (a) an interaction with constant matrix elements of magnitude $G \approx 25/A$ MeV, (b) a contact interaction of strength $\frac{294}{4\pi}$ MeV fm^2, (c) an effective two-body force (Gogny (1975), Skyrme (1959)) whose parameters were adjusted so as to reproduce nuclear observables.

Although these calculations have shed much light on the workings of pairing correlations in nuclei, they say little concerning the relative importance of the bare nucleon–nucleon interaction and of the many-body renormalization effects taking place in the atomic nucleus. To gain insight into this question one has to proceed in several steps, starting with the bare nucleon–nucleon interaction, adding the renormalization effects afterwards. It has to be remembered that the results are not expected to be a simple sum of the different contributions, as the problem is highly non-linear. Making use of an analogy one can think of a metal, and of the non-linear effects associated with the simultaneous treatment of the bare Coulomb interaction, the coupling of electrons to plasmons (screening) and the coupling of electrons to phonons (Cooper pair formation) (see, e.g. Broglia *et al.* (2004)).

In the following three chapters we shall show that the nuclear surface plays a central role in the pairing phenomenon. This is due to the renormalization effects arising from the coupling of nucleons to low-lying collective surface vibrations. The most important effects are: the dressing of particles leading to an effective mass, and the exchange of vibrations among nucleons, giving rise to an induced pairing interaction. By taking all these effects into account on equal footing with the bare nucleon–nucleon interaction a consistent picture of pairing in nuclei is obtained (see Section 10.4 and Chapter 11).

The present chapter is an introduction to the renormalization problem. The contribution of the bare nucleon–nucleon (NN) interaction to the pairing gap is discussed in Sections 8.1 and 8.2. Calculations with a local single-particle

170

potential give a pairing gap in agreement with experiment, but non-local effects reduce this by a factor of 2 (see Figs. 8.6 and 8.9). This is because the effective k-mass $m_k \sim 0.7m$ increases the spacing of single-particle levels near the Fermi surface. The role of the non-local effects is analysed in Section 8.2 (see Appendices B and E and H, Section H.4) with the conclusion that coupling of single-particle motion to low-energy collective modes must lead to important renormalization effects. Section 8.3 contains an introduction to particle-vibration coupling (see Appendices D and H, Section H.4) and the microscopic description of both low-energy and high-energy (giant resonances) collective modes.

Chapter 9 is concerned with the dynamical shell model. Coupling of single-particle motion to surface vibrations gives a time-dependent component to the nucleon–nucleus interaction which manifests itself as an energy dependence in the shell model potential. This energy dependence can be incorporated in the ω-mass $m_\omega > m$ which modifies the effects of the k-mass, and also of the occupation factors (see Appendix E and Section H.4).

The remaining contribution of the particle-vibration coupling is included in an effective interaction due to the exchange of surface phonons. The renormalized interaction is studied in Chapter 10 for the case of nuclei lying along the stability valley and in Chapter 11 for halo (exotic) nuclei.

8.1 The bare nucleon–nucleon potential and the pairing interaction

While one does not know how to work out a reliable nucleon–nucleon interaction at the level of quarks and gluons, phenomenological nucleon–nucleon interactions exist which describe quite accurately the variety of phase shifts obtained from the analysis of scattering processes in isolated two-nucleon systems (e.g. np and pp systems) and arising from the exchange of mesons, the carriers of the strong interaction. In the present context we are interested in the $^{2S+1}L_J = {}^1S_0$ phase shift, observed in the s-wave channel in the scattering of two identical ($T = 1$) nucleons in a singlet spin state.

This phase shift, shown in Fig. 8.1, is large and positive (implying an attractive interaction) at low relative momenta (typical, in the case of the atomic nucleus, of the surface region). It decreases as the relative momenta increase becoming zero and eventually negative (repulsive interaction) at relative momenta typical of nuclear saturation density.

Conventional models of the NN interaction are based on non-relativistic protons and neutrons interacting via a two-body potential. Typical NN potentials contain a strong short-range repulsion, an intermediate-range attraction, and a long-range one-pion-exchange (OPE) part (see Fig. 8.2(a)). One knows that such an approach is a great simplification over reality. Nucleons are composite systems with a rich resonance structure, which can be attributed to constituent quarks interacting by gluon exchange. Ideally a model of the NN interaction
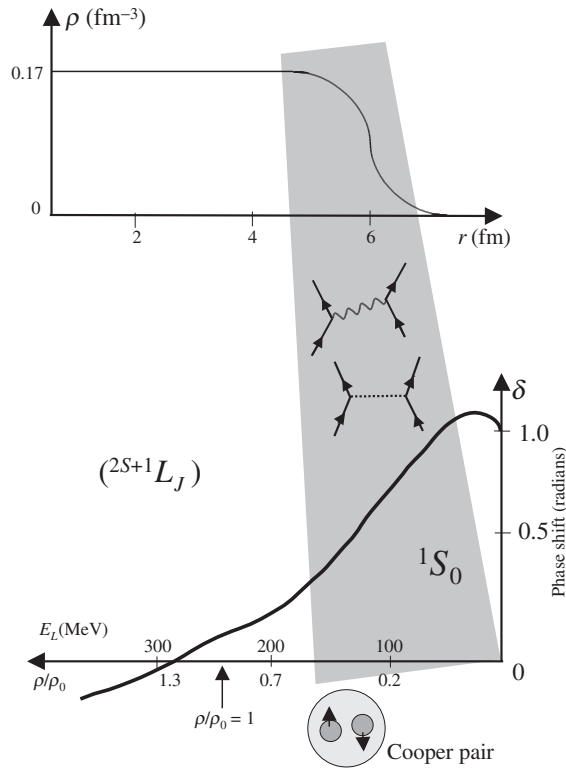
Figure 8.1. (Top) Schematic representation of the nuclear density ρ in units of fm^{-3} plotted as a function of the distance r (fm) from the centre of the nucleus. (Bottom) Phase shift δ associated with the elastic scattering of two nucleons moving in a singlet state of spin zero. Positive values of δ imply an attractive interaction, negative a repulsive one. For kinetic energies E_L associated with low relative velocities, i.e. around the nuclear surface where the density is low, the $^1S_0$ phase shift arising from the exchange of mesons (for example pions, represented by a horizontal dotted line in the scattering diagrams) between nucleons (represented by upward pointing arrowed lines) is attractive, and nucleons moving in time-reversal states form Cooper pairs which eventually condense leading to nuclear superfluidity. This effect is further accentuated because of the exchange of collective surface vibrations (wavy line in the scattering process) between the members of the Cooper pair.

would start with a field theoretical description of quark–quark interactions, but no satisfactory theory has yet been developed.

The Argonne v_{14} potential (Wiringa *et al.* (1984)) provides a convenient parametrization of the NN interaction to be used in nuclear structure calculations. It has the form

$$v_{14}(ij) = \sum_{p=1,14} [v_\pi^p(r_{ij}) + v_{\mathrm{I}}^p(r_{ij}) + v_{\mathrm{s}}^p(r_{ij})]O_{ij}^p, \tag{8.1}$$
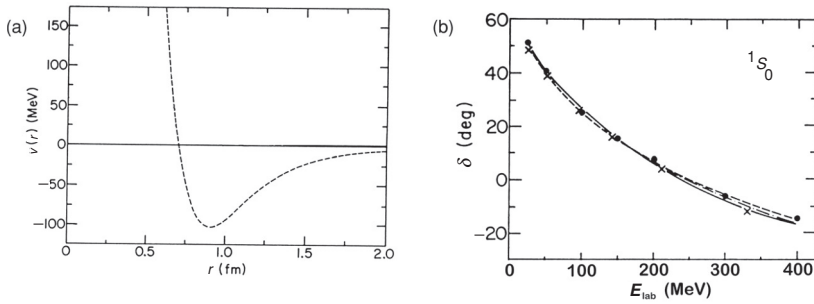
Figure 8.2. (a) $T = 1$, $S = 0$ central potential associated with the v_{14} NN interaction. (b) $T = 1$, $S = 0$ $^1S_0$ phase shifts: solid lines and dots are the energy-dependent and energy-independent phases of Arndt and Roper (1985). The dashed curve is the v_{14} model phase shift. Reprinted with permission from Wiringa *et al.*, *Phys. Rev.* **C29**: 1207–21 (1984) Copyright 1984 by the American Physical Society.

where

$$O_{i,j}^{p=1,14} = 1, \vec{\tau}_i \cdot \vec{\tau}_j, \vec{\sigma}_i \cdot \vec{\sigma}_j, (\vec{\sigma}_i \cdot \vec{\sigma}_j)(\vec{\tau}_i \cdot \vec{\tau}_j), S_{ij}, S_{ij}(\vec{\tau}_i \cdot \vec{\tau}_j),$$
$$(\vec{L} \cdot \vec{S}), (\vec{L} \cdot \vec{S})(\vec{\tau}_i \cdot \vec{\tau}_j), \vec{L}^2, \vec{L}^2(\vec{\tau}_i \cdot \vec{\tau}_j), \vec{L}^2(\sigma_i \cdot \sigma_j),$$
$$\vec{L}^2(\vec{\sigma}_i \cdot \vec{\sigma}_j)(\vec{\tau}_i \cdot \vec{\tau}_j), (\vec{L} \cdot \vec{S})^2, (\vec{L} \cdot \vec{S})^2(\vec{\tau}_i \cdot \vec{\tau}_j). \tag{8.2}$$

Here

$$S_{ij} = 3(\sigma_i \cdot \hat{r}_{ij})(\sigma_j \cdot \hat{r}_{ij}) - \vec{\sigma}_i \cdot \vec{\sigma}_j \tag{8.3}$$

is a tensor operator, $\vec{L}$ is the relative orbital angular momentum, and $\vec{S}$ is the total spin of the pair.

The first eight operators of equation (8.2) are the standard ones required to fit singlet and triplet S- and P-wave data. The 14 operators provide sufficient freedom to characterize the 14 singlet and triplet S, P, D and F states. The three radial components include the long-range OPE part v_π^p, and phenomenological intermediate-range and short-range parts $v_I^p(r)$, $v_s^p(r)$. As an example we show in Fig. 8.2(a) the $T = 1$, $S = 0$ central potential. The Argonne v_{14} $^1S_0$ phase shift fits for the experimental data (see Fig. 8.2(b)) are quite good with only one short-range functional form.

8.1.1 Calculation of the pairing properties of ^{120}Sn

Hartree–Fock–Bogoliubov-like calculations (Thouless (1961a,b), Ring and Schuck (1980)) of the pairing properties of the semi-magic nucleus $^{120}_{50}Sn_{70}$ have been carried out by Barranco *et al.* (1997), allowing the neutrons to move in the single-particle states of a Saxon–Woods potential (with parameters $V^0 = -55$ MeV, $r_0 = 1.2$ fm, $a = 0.65$ fm) and interacting through a v_{14}

NN interaction. By solving the matrix equation

$$\begin{pmatrix} \varepsilon_i - \lambda & \Delta \\ \Delta & -(\varepsilon_i - \lambda) \end{pmatrix} \begin{pmatrix} U_i \\ V_i \end{pmatrix} = E_i \begin{pmatrix} U_i \\ V_i \end{pmatrix} \tag{8.4}$$

self-consistently with the constraint

$$N = 2 \sum_{a_1 > 0} V_i{}^2, \tag{8.5}$$

which fixes the average number of particles of the system and the Fermi energy λ, one obtains the quasiparticle energies E_i and occupation amplitudes V_i and U_i. The state-dependent pairing gap

$$\Delta_{a_1 a_2} = -\frac{1}{2} \sum_{b_1 b_2} \sum_i U_{b_1}^i V_{b_2}^i \langle a_1 \tilde{a}_2 | v_{14} | b_1 \tilde{b}_2 \rangle, \tag{8.6}$$

with $a_1 \equiv (n_1(l_1 1/2) j_1, m_1)$, where n_1, l_1, j_1 and m_1 are the number of modes, the orbital, the total angular momentum and its projection respectively of the state $|a_1\rangle$, depends on the matrix elements between two-particle states with the same or different number of nodes. The state $|\tilde{a}_2\rangle$ is obtained from the state $|a_2\rangle$ by the operation of time reversal.

As seen from the expression for the quasiparticle energy

$$E_{a_1} = \sqrt{(\varepsilon_{a_1} - \lambda)^2 + \Delta_{a_1 a_1}^2},$$

the quantity $\Delta_{a_1 a_2}$ is an energy gap in the spectrum of quasiparticles in the case of a continuous spectrum. For a discrete spectrum, it is meaningful to speak of a gap only for values of $\Delta_{a_1 a_2}$ which are greater than the distances between the single-particle energies ε_{a_1}.

Equations (8.4) and (8.5) always have a trivial solution, namely $\Delta_{a_1 a_2} = 0$ and $U_{a_1} = 1$, $V_{a_1} = 0$ for $\varepsilon_{a_1} > \lambda$ and $U_{a_1} = 0$, $V_{a_1} = 1$ for $\varepsilon_{a_1} < \lambda$. However, if the inequality

$$-\frac{1}{2} \sum_{b_1 b_2} \frac{\langle a_1 \tilde{a}_2 | v_{14} | b_1 \tilde{b}_2 \rangle}{\sqrt{|\varepsilon_{b_1} - \lambda||\varepsilon_{b_2} - \lambda|}} > 1 \tag{8.7}$$

is fulfilled, then there is also a non-trivial ($\Delta_{a_1 a_1} \neq 0$) solution of equations (8.4) and (8.5). This is possible only if the pairing component of the NN potential has a coherent character for sufficiently many states. In other words, the matrix elements $\langle a_1 \tilde{a}_2 | v_{14} | b_1 \tilde{b}_2 \rangle$ must have the same sign for a sufficiently broad region of states. If this is not the case cancellations will occur and coherence will be lost (Belyaev (1959)).
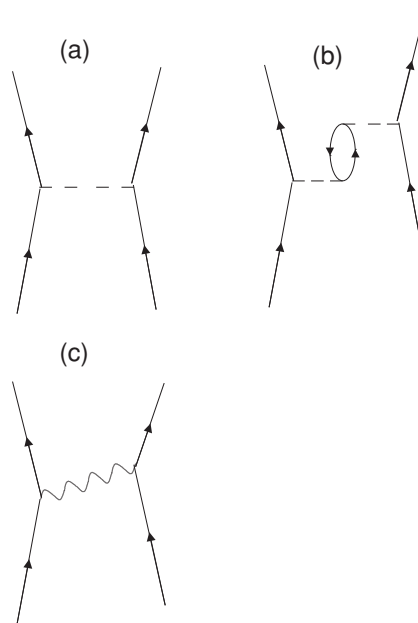
Figure 8.3. (a) NN scattering process through a bare interaction (horizontal dashed line; nucleons are drawn as arrowed lines). (b) Renormalization of the bare NN interaction due to core polarization (single particle–hole excitation, bubble). (c) NN interaction arising from the exchange of a collective vibration (resulting from bubble process summed to all orders (RPA), see Section 8.3).

Expanding the two-body interaction potential in spherical harmonics (see Fig. 8.3)

$$v_{14}(|\vec{r}_1 - \vec{r}_2|) = \sum_L v^L(r_1, r_2) P_L(\cos\theta_{12}),$$

helps to understand which parts of the NN interaction contribute to a coherent pairing interaction (see also Section 2.2). The spherically symmetric or monopole part of the interparticle interaction contributes to the self-consistent field. The single-particle levels in this field are degenerate and characterized by the value of the angular momentum j. Let us consider the particles in the same level j and neglect the interaction with the particles in other shells. The low-multipolarities ($L \lesssim 3$–5) are not expected to contribute to the pairing interaction in any substantial way, because they connect the levels with similar magnetic quantum numbers $|m_{a_1} - m_{b_1}| \leq L \approx 3$–5 and do not contribute in a significant way to the inequality equation (8.7). Therefore, the main contribution to the pairing interaction associated with the bare interaction comes from the high harmonics of the NN potential. This is the standard argument made in connection with pairing in nuclei (see e.g. Belyaev (1959), Mottelson (1962, 1996)).

On the other hand, low multipolarities give essential contributions to the mean field. In particular $L = 2$, 3 and 4 can lead to spheroidal, octupole and hexadecapole static or dynamic (surface vibration) distortions. The low multipole components of the bare NN interaction give a small contribution to the pairing force, but the renormalization effects arising from core excitation (polarization) processes (Fig. 8.3(b)) are expected to be important (Bohr and Mottelson (1975), Section 6-5f). This is because such processes receive coherent contributions from all orders of perturbation (many-bubble processes), leading to collective surface vibrations of low energy which couple strongly to the nucleons (see Fig. 8.3(c)).

To obtain convergence of the solutions to equations (8.4) and (8.6), jumps of pairs of nucleons to single-particle orbitals lying as high as 600 MeV from ε_F have to be included in the calculations. For this purpose the continuum is discretized by placing the nucleus in a box. The size of the box is to be changed until convergence of the results is obtained. In the case of ^{120}Sn this is achieved for $R_{box} \geq 12$ fm.

The large value of the energy associated with the two-particle scattering processes contributing to $\Delta_{a_1 a_2}$ is essentially due to the strong repulsion of the $T = 1$, $S = 0$ central potential (see Fig. 8.2) and not to the fact that the most important contribution to Cooper pair formation is connected with the high multipoles of the residual interactions, as discussed in connection with the condition given in equation (8.7). In fact, as seen from the single-particle valence spectrum of ^{120}Sn (see Fig. 8.4), levels with total spin as high as 11/2 and 9/2 are already present in this subspace, thus allowing the particles to profit from the v_{14} pairing correlations within this restricted subspace. This fact can be better appreciated from Fig. 8.5 where typical examples of the pairing matrix elements $\langle (a_1 a_2)_0 | v_{14} | (b_1 b_2)_0 \rangle$ are shown as a function of the energy associated with the (NN) scattering process. The negative (attractive) matrix elements are all concentrated at low energies (<20 MeV), associated essentially with scattering processes among valence single-particle orbits.

In Fig. 8.6 we show the diagonal part of the neutron pairing gap Δ_{a_k} ($\equiv \Delta_{a_k a_k}$) associated with the single-particle states of the system (Barranco *et al.* (1997)). The results have been averaged over an energy interval of ≈ 1 MeV to smooth out fluctuations associated with particular shells. The value of the pairing gap at the Fermi energy is $2.2^{+0.4}_{-0.8}$ MeV, the 'errors' reflecting the conspicuous state dependence of Δ. This value is of the same order of magnitude as that extracted from the odd–even mass difference, namely 1.4 MeV. One would then be tempted to conclude that the bare NN potential explains, even quantitatively, the values of the odd–even mass difference observed experimentally, and thus pairing superfluidity in nuclei. As we shall show below, this conclusion is not correct.
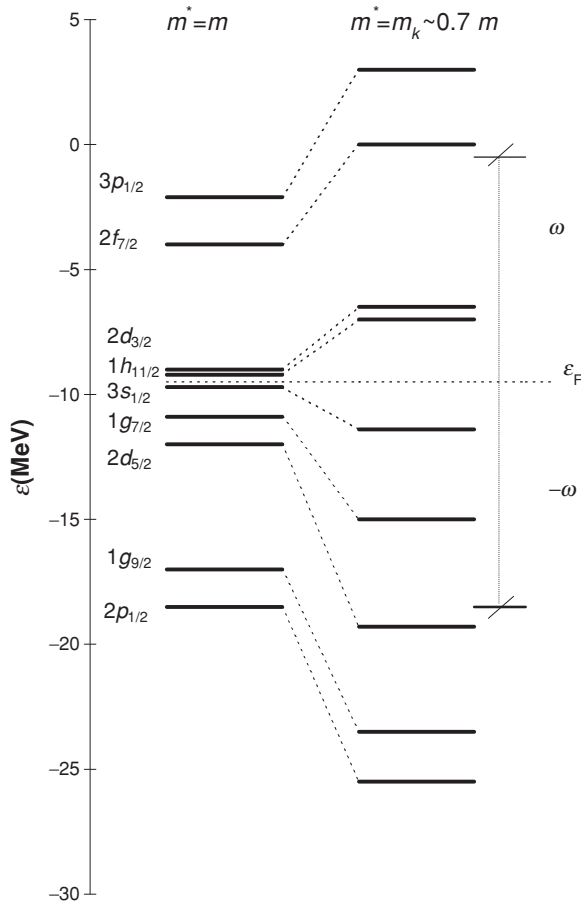
Figure 8.4. Valence single-particle levels used in the calculation of the pairing parameters of ^{120}Sn, determined using a Saxon–Woods potential with parameters given in equations (8.13)–(8.16) ($V = V^0 = -55$ MeV), and two effective k-masses (see equations (8.19) and (8.20)). The value of the Fermi energy $\varepsilon_F (\equiv \lambda)$ was obtained by solving the BCS number and gap equations with $N = 70$. Also indicated is the energy interval $\pm\omega$ around the Fermi energy over which the density of levels $N(0)$ is calculated (see the discussion following equation (8.20)).

8.2 Mean-field theory

Both in previous chapters as well as in solving the matrix eigenvalue relation given in equation (8.4), the assumption has been made that nucleons move in a local single-particle potential. This is, however, not correct. The equations which have to be solved to determine the single-particle energies and the occupation amplitudes consistently, are the integro-differential Hartree–Fock–Bogoliubov
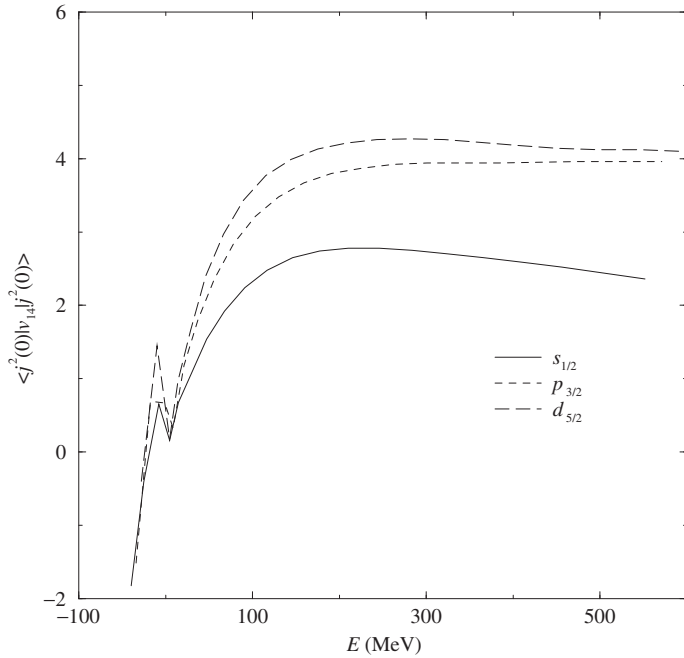
Figure 8.5. Diagonal matrix elements $\langle (n_1 l_1 j_1, n_2 l_1 j_1) 0^+ | v_{14} | (n_1 l_1 j_1, n_2 l_1 j_1) 0^+ \rangle$ of the v_{14} NN potential associated with $s^2(0)$, $p^2(0)$ and $d^2(0)$ configurations of ^{120}Sn, as a function of the energy involved in the scattering process. The negative values are associated with states involving low relative momentum and thus feeling mainly relative distances $r \gtrsim 0.8$ fm. Those associated with positive values are associated with states involving high relative momenta and thus probing the repulsive core (see Fig. 8.2(a)) (This figure is due to F. Barranco and E. Vigezzi).
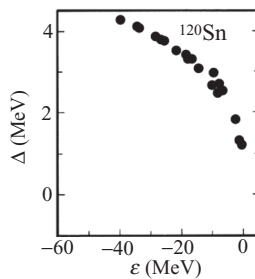

Figure 8.6. The state-dependent diagonal pairing gap of ^{120}Sn calculated making use of equations (8.4) and (8.5) and of the v_{14} matrix elements of the type shown in Fig. 8.5. The relation given in equation (8.5) for $N = 70$ fixes the Fermi energy at $\varepsilon_F = -7.2$ MeV.

equations, containing both a local (Hartree) and a non-local (Fock) potential. In other words, equation (8.4) has to be supplemented so as to be able to calculate self-consistently the single-particle energies ε_i. In the following we derive the corresponding equations.

Mean-field theory is a very useful approximation in the study of the many-particle system. In the mean-field method one replaces the many-particle Schrödinger equation,

$$\left(-\sum_{i=1}^{A} \frac{\hbar^2}{2m} \nabla_i^2 + \sum_{i<j=1}^{A} v(|\vec{r}_i - \vec{r}_j|) \right) \Psi_n(\vec{r}_1 \ldots \vec{r}_A) = E_n \Psi_n(\vec{r}_1 \ldots \vec{r}_A), \quad (8.8)$$

by a single-particle Schrödinger equation,

$$\left(-\frac{\hbar^2}{2m} \nabla^2 + U(r) \right) \varphi_{v_j}(\vec{r}) + \int d^3\vec{r}' U_x(\vec{r}, \vec{r}') \varphi_{v_j}(\vec{r}') = \varepsilon_{v_j} \varphi_{v_j}(\vec{r}) \quad (8.9)$$

and the total wavefunction $\Psi_n(\vec{r}_1 \ldots \vec{r}_A)$ by the normalized determinant constructed out of the single-particle wavefunctions $\varphi_i(\vec{r})$.

The two potentials appearing in equation (8.9) are the Hartree (direct) potential,

$$U(\vec{r}) = \int d^3\vec{r}' \varrho(\vec{r}') v(|\vec{r} - \vec{r}'|), \quad (8.10)$$

where

$$\varrho(\vec{r}) = \sum_{v_i \leq v_F} |\varphi_{v_i}(\vec{r})|^2$$

is the total density of the system, and the Fock (exchange) potential

$$U_x(\vec{r}, \vec{r}') = -\sum_{v_i \leq v_F} \varphi_{v_i}^*(\vec{r}') v(|\vec{r} - \vec{r}'|) \varphi_{v_i}(\vec{r}). \quad (8.11)$$

This last term is directly connected with the fact that nucleons are fermions and thus satisfy the Pauli principle. In particular, the exchange potential ensures that nucleons do not interact with themselves (see Appendix A).

The total energy of the system in the Hartree–Fock ground state $|0\rangle_{\mathrm{HF}} = \frac{1}{\sqrt{A!}} \det(\varphi_{v_1}(\vec{r}_1) \ldots \varphi_{v_A}(\vec{r}_A))$ is given by

$$E = {}_{\mathrm{HF}}\langle 0|H|0\rangle_{\mathrm{HF}} = \sum_{v_i \leq v_F} \langle v_i|T|v_i\rangle + \frac{1}{2} \sum_{v_i, v_{i'} \leq v_F} \langle v_i v_{i'}|v|v_i v_{i'}\rangle_a$$

$$= \sum_{v_i \leq v_F} \varepsilon_i - \frac{1}{2} \sum_{v_i, v_{i'} \leq v_F} \langle v_i v_{i'}|v|v_i v_{i'}\rangle_a, \quad (8.12)$$

where v_F labels the Fermi level lying, by definition (zero temperature situation), halfway between the last occupied and the first unoccupied orbitals. In writing

up the last term of the above equation the self-consistency relation

$$\langle v_2|T|v_1\rangle + \sum_{v_i \leq v_F} \langle v_i v_2|v|v_i v_1\rangle_a = \langle v_2|T + U + U_x|v_1\rangle = \varepsilon_{v_1}\delta(v_1, v_2),$$

i.e. the matrix expression of equation (8.9), has been used. Note that the subindex a in the matrix element indicates the antisymmetrized matrix element, i.e. $\langle v_i v_k|v|v_i v_k\rangle_a = \langle v_i v_k|v|v_i v_k\rangle - \langle v_i v_k|v|v_k v_i\rangle$, and thus gives rise to both the direct and exchange potentials (see equation (A.16)). The factor $\frac{1}{2}$ in the last term of equation (8.12) reflects the fact that the two-particle interaction contributes to the average potential for both of the interacting particles and is thus counted twice, if one sums the single-particle energies for the filled orbitals (see equation (3.50)).

8.2.1 Effective mass (k-mass)

There is extensive experimental evidence showing that single-particle motion in nuclei is well described by a potential of Saxon–Woods type,

$$U(r, E) = V_0(E)f(r), \tag{8.13}$$

where

$$f(r) = \frac{1}{1 + \exp(\frac{r - R_0}{a})}, \tag{8.14}$$

to which a spin-orbit potential, proportional to $\frac{\partial f(r)}{\partial r}$, is added (see Bohr and Mottelson (1969)). The radius and the diffuseness parameters have the values

$$R = r_0 A^{\frac{1}{3}} \text{ fm}, \quad r_0 = 1.2 \text{ fm}, \quad a = 0.65 \text{ fm}, \tag{8.15}$$

and, for levels around the Fermi energy (valence orbitals), the strength $V_0(E)$ is a constant. On the other hand, the differential elastic scattering cross-section and the total nucleon–nucleus cross-section can be accurately described by

$$V = V_0(E) = V^0 + V_1 \frac{N - Z}{A} + \gamma E, \tag{8.16}$$

with $V^0 = -55$ MeV, $\gamma = 0.3-0.4$ and $V_1 \approx 30$ MeV, provided that one adds to the potential given in equation (8.13) an imaginary component (see Appendix B). The same parametrization describes the deeply bound states as shown in Fig. 8.7.

The relation given in equation (8.16) is valid for $|E| > 10$ MeV, where the single-particle energy $E (= \varepsilon - \varepsilon_F)$ is measured from the Fermi energy. The valence orbitals ($|E| \leq 5$ MeV) of nuclei around closed shells are well reproduced by the Saxon–Woods potential defined by equations (8.13)–(8.15) but in this case with $V \approx -55$ MeV, independent of energy.
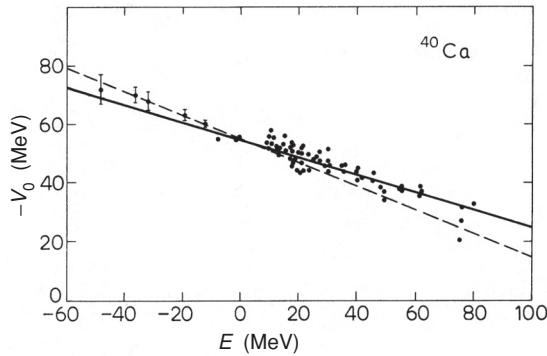
Figure 8.7. Dependence upon proton-bombarding energy of the depth V_0 of the potential well (defined in equation (8.13)) which reproduces the ^{40}Ca(p, p) differential cross-section for $E > 10$ MeV, and the experimental single-proton energies for $E < 0$ MeV. The full straight line corresponds (in MeV) to $V = V_0(E) = -55$ MeV $+ 0.3E$, and the dashed straight line to $V = V_0(E) = -55$ MeV $+ 0.4E$ (adapted from Bauer *et al.* (1982)).

The Schrödinger equation (8.9) can, for many purposes, be rewritten to a good approximation as (Mahaux *et al.* (1985))

$$\left(-\frac{\hbar^2}{2m_k}\nabla^2 + \tilde{U}(r)\right)\varphi_j(\vec{r}) = \varepsilon_j\varphi_j(\vec{r}) , \qquad (8.17)$$

where the k-effective mass m_k, which takes into account many of the effects associated with the non-local Hartree–Fock potential, has been introduced, and where the depth of the potential $\tilde{U}(r)$ is

$$\tilde{V}^0 = \frac{m}{m_k}V^0. \qquad (8.18)$$

As shown in Appendix B (note that m_k may depend on r),

$$m_k = m\left(1 + \frac{m}{\hbar^2 k}\frac{\partial V(k)}{\partial k}\right)^{-1} , \qquad (8.19)$$

where $V(k)$ is the Fourier transform of the Fock potential given in equation (8.11).

In Hartree–Fock theory, contributing to the energy dependence of the single-particle potential are the non-locality of $U_x(\vec{r}, \vec{r}')$, equivalent to a dependence on the linear momentum of the particle, and, in many cases, the genuine velocity-dependence of the two-body interaction. Equation (8.19) with the parametrization given in equation (8.16) leads to an effective mass $m^* = m_k$, known as the k-mass, which is considerably smaller than the bare nuclear mass. In fact,

$$m_k \approx 0.6m \rightarrow 0.7m. \qquad (8.20)$$

Consequently, Hartree–Fock theory is able to accurately predict the sequence of the single-particle levels around the Fermi energy (i.e. $|E| \leq 10$ MeV), but not its
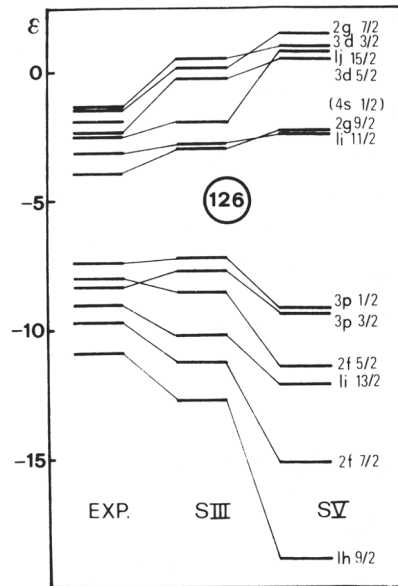
Figure 8.8. Comparison between the experimental single-neutron energies in the valence shells of ^{208}Pb and the values calculated in the Hartree–Fock approximation with a Skyrme III (SIII, middle) and a Skyrme V (SV, right) interaction (taken from Quentin and Flocard (1978)).

density. This is exemplified in Fig. 8.8 (see also Fig. 8.4), where the experimental values of the single-particle neutron energies of the valence orbitals of ^{208}Pb are compared with Hartree–Fock results calculated by making use of a particular parametrization of the effective two-body interaction (all displaying an effective k-mass smaller than the bare mass).

Making use of the k-mass given in equation (8.20) to calculate the single-particle energies appearing in equations (8.4), i.e. the solution of equation (8.17) with $m_k \approx 0.7m$ and with $\tilde{U}(r) = \tilde{V}^0 f(r)$, one obtains $\Delta_{a_1} \approx 0.5$ MeV (Barranco *et al.* (2004); see Fig. 8.9). This result, compared with the result shown in Fig. 8.6, can be understood by studying the dependence of the gap on the density of levels. For this purpose we make use of the results of the single j-shell. In this case the pairing gap has a simple expression in term of the pairing coupling constant G, the number of particles N and the pair dependency $\Omega = (2j + 1)/2$. For a half-filled shell ($N = \Omega$) (see Appendix H)

$$\Delta = \frac{1}{2}G\Omega \approx \frac{G}{2}N(0)\omega, \tag{8.21}$$

where $N(0) = 2\Omega/2\omega$ is the density of levels at the Fermi energy, and where 2ω is the range of energy around the Fermi energy where pairs of particles
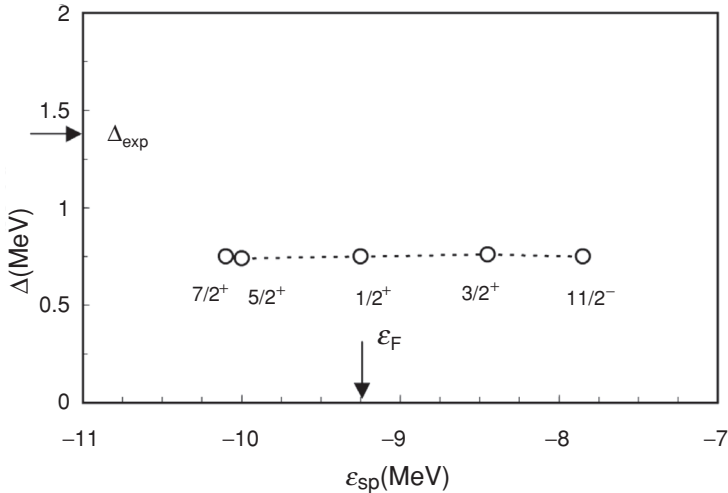
Figure 8.9. The state-dependent pairing gap of ^{120}Sn for the levels close to the Fermi energy obtained using BCS theory with the v_{14} Argonne potential (after Barranco *et al.* (2004)).

coupled to angular momentum zero are allowed to correlate through the pairing interaction. In the case under discussion and making use of a typical value of $\omega = 8\,\text{MeV}$ (see Fig. 8.4), the density of levels (for one spin orientation) changes from $N(0) = 3.4\,\text{MeV}^{-1}$ ($m^* = m$) to $N(0) = 1.6\,\text{MeV}^{-1}$ ($m^* = m_k = 0.7m$) (see (3.61) and (3.62)). Thus, the simple relation given in equation (8.21) predicts a decrease of a factor of 2 in the pairing gap. Among the limitations of Hartree–Fock theory to describe the nuclear structure one can mention: low density of levels, unrealistic occupation factors with values of either 1 or 0, single-particle states with infinite lifetimes (neglecting electromagnetic decay). These limitations are connected with the fact that HF is a static approximation to the many-body problem. That is, an approximation where fluctuations of the different (order) parameters characterizing the mean field are neglected (see e.g. equation (4.8) and subsequent discussion).

The presence of a mean field defines a surface which can vibrate. The vibrations renormalize (by coupling to the nucleons) their properties, giving rise to an effective mass (so-called ω-mass m_ω), to occupation factors $Z_\omega = (m/m_\omega)$ as well as to a splitting of the single-particle strength. The corresponding energy spread Γ_ω determines the lifetime ($\hbar/\Gamma_\omega$) of the single-particle levels. These phenomena affect pairing correlations in an important, and sometimes opposite way. In particular, particles which have to carry a phonon for part of the time become effectively heavier than free particles. This leads to levels which are closer to the Fermi energy, and to an increase of the level density over that of HF theory (see Chapter 9 and Appendix B). The increase of the level density leads to an increase of the pairing gap. On the other hand, the fact that nucleons are

for part of the time in configurations containing a phonon means that the bare nucleon–nucleon interaction is less effective, leading to a decrease of the pairing correlations. This decrease is accentuated due to the fact that single-particle levels acquire an effective width due to the coupling to phonons (see equation (9.41)).

A phonon need not be reabsorbed by the same nucleon which has virtually excited it, but can be exchanged between pairs of nucleons. If these two nucleons move in time-reversal states, this exchange leads to an effective pairing interaction and thus to an increase of the pairing gap, because the degrees of freedom of the nucleons and of the collective vibrations overlap to some extent and one has to eliminate processes which are due to overcompleteness of the basis (see e.g. Appendix F).

Summing up, the interweaving of particles and vibrations affects pairing correlations in nuclei in a subtle way. This subject is discussed in Chapters 10 and 11.

In what follows we develop the tools to carry out this discussion. That is, we work out the particle-vibration coupling Hamiltonian. The general rules needed to calculate the variety of processes arising from the interweaving of nucleons and vibrations are discussed in Chapter 9 and Appendix D.

8.3 Random phase approximation

In solving the Hartree–Fock equations one has to specify the shape of the nucleus. The absolute minimum of the energy of a closed-shell system is associated with a spherical configuration. For nuclei with a number of nucleons outside the closed shell, or a number of holes in the closed shell, the absolute minimum may correspond to a deformed configuration. In either case there can be vibrations about the equilibrium shape which couple to the single-particle motion. The present section introduces the theory of particle-vibration coupling when the mean field is spherical. This leads to a microscopic description of the low-energy surface vibrations in the random phase approximation. The approach in this section is based on the one developed by Bohr and Mottelson (1975).

There is a simple parametrization of the nuclear radius which can account for the variety of situations. It is given by

$$R = R_0 \left(1 + \sum_{\lambda\mu} \alpha_{\lambda\mu} Y^*_{\lambda\mu}(\hat{r}) \right), \tag{8.22}$$

with the multipolarity $\lambda \geq 2$ and where $\alpha_{\lambda\mu}$ are deformation parameters while $Y_{\lambda\mu}$ are spherical harmonics. An adequate parametrization of the potential is still provided by equation (8.14), but with R_0 replaced by R. In the case of axially symmetric quadrupole deformations, the only deformation parameter different from zero is α_{20}. The Nilsson model used to describe the single-particle motion

in quadrupole deformed nuclei is closely related to this potential (see Nilsson (1955) and Nilsson and Ragnarsson (1995)).

Let us now expand the single-particle potential to first order in the deformation parameters ($\alpha^2 \ll \alpha$). One obtains

$$U(r, R) = U(r, R_0) + \delta U(r), \tag{8.23}$$

where

$$\delta U(r) = -R_0 \frac{\partial U}{\partial r} \sum_{\lambda \mu} \alpha_{\lambda \mu} Y^*_{\lambda \mu}(\hat{r}). \tag{8.24}$$

It is well established that the nuclear surface can vibrate in certain normal modes. In this case the quantities $\alpha_{\lambda \mu}$ can be viewed as the coordinates of the harmonic oscillator Hamiltonian associated with the normal modes, i.e.

$$H_\alpha = \frac{\hat{\Pi}^2_\alpha}{2 D_\alpha} + \frac{C_\alpha}{2} \hat{\alpha}^2, \tag{8.25}$$

where

$$\hat{\alpha} = \sqrt{\frac{\hbar \omega_\alpha}{2 C_\alpha}} (\hat{\Gamma}^\dagger_\alpha + \Gamma_\alpha), \tag{8.26}$$

and $\hat{\Pi}_\alpha$ is the momentum variable conjugate to $\hat{\alpha}$. The quantities $\Gamma^\dagger_\alpha$ and Γ_α are boson creation and annihilation operators (Dirac (1935)) of the vibrational modes. Here $\omega_\alpha = \sqrt{C_\alpha / D_\alpha}$ and the quantity $\sqrt{\hbar \omega_\alpha / 2 C_\alpha}$ is the amplitude of the zero-point fluctuations in the ground state (the boson vacuum state $|0\rangle_B$). The one-phonon state is

$$|\alpha\rangle = \Gamma^\dagger_\alpha |0\rangle_B, \tag{8.27}$$

(see Appendix A). Consequently, the term δU leads to a coupling between the single-particle motion described in terms of the coordinate $\vec{r}$, and the collective vibrations, described in terms of the collective coordinates $\hat{\alpha}$, which we write as

$$\delta U = -\kappa \hat{\alpha} \hat{F}, \tag{8.28}$$

where κ is a coupling strength,

$$\hat{F} = \sum_{\nu_1 \nu_2} \langle \nu_1 | F | \nu_2 \rangle a^\dagger_{\nu_1} a_{\nu_2}, \tag{8.29}$$

and $a^\dagger_{\nu_1}$ and a_{ν_2} are creation and annihilation operators of single-particle states. The dimensionless quantity

$$F = \frac{R_0}{\kappa} \frac{\partial U}{\partial r} Y^*_{\lambda \mu}(\hat{r}) \tag{8.30}$$
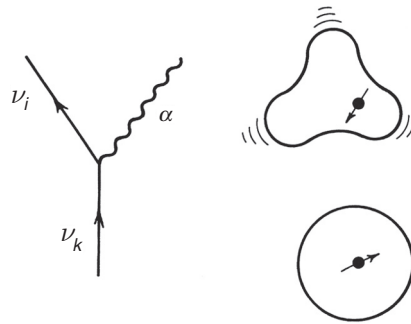
Figure 8.10. Graphical representation of the process by which a fermion, bouncing inelastically off the surface, sets it into vibration. Particles are represented by an arrowed line, while the vibration is shown by a wavy line. The black dot represents a nucleon moving in a spherical mean field of which it excites an octupole vibration after bouncing inelastically off the surface.

is a single-particle field peaked at the nuclear surface. In a normal self-sustained mode, there should be a consistency between variations of the density and of the potential. This is a generalization of the self-consistent condition existing between potential and density in the static case (see equation (8.10)) As we shall see in Sections 8.3.1 and 8.3.3, the quantity κ is the proportionality constant between these two variations.

Here we are treating angular momentum in a very cavalier way. This is done in order to be able to discuss the main physical consequences of the particle-vibration coupling Hamiltonian defined in equation (8.28) in simple terms. We refer the reader to Bohr and Mottelson (1975) and Bortignon *et al.* (1977) for the detailed expressions containing the proper angular momentum coupling coefficients (see also Chapter 10 and Appendix D).

The basic process described by the particle-vibration coupling Hamiltonian δU is that of a particle scattering inelastically off the surface and setting it into vibration, as shown in Fig. 8.10. The ease with which the process takes place is measured by the matrix element between the single-particle state $|\nu_k\rangle$ and the state $|\alpha \nu_{k'}\rangle$ representing a single particle coupled to a phonon
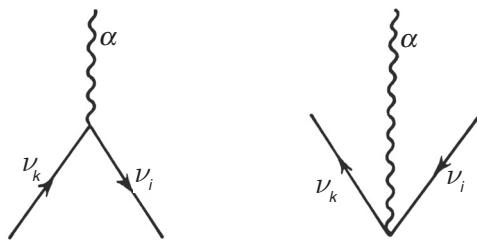
$$V(\nu_k, \nu_{k'}; \alpha) = \langle \alpha \nu_{k'} | \delta U | \nu_k \rangle = \Lambda_\alpha \langle \nu_k' | \hat{F} | \nu_k \rangle. \tag{8.31}$$

Here

$$\Lambda_\alpha = -\kappa \sqrt{\frac{\hbar \omega_\alpha}{2 C_\alpha}} = \frac{-\kappa \beta_{\lambda \alpha}}{\sqrt{2 \lambda_\alpha + 1}} \tag{8.32}$$

is the strength with which the particle couples to the vibration, and

$$\langle \nu_k' | \hat{F} | \nu_k \rangle = \int \mathrm{d}^3 r \, \varphi_{\nu_k'}^*(\vec{r}) F(\vec{r}) \varphi_{\nu_k}(\vec{r}), \tag{8.33}$$

Figure 8.11. Graphical representation of two matrix elements of δU.

where $\varphi_{\nu_k}(\vec{r})$ and $\varphi_{\nu'_k}(\vec{r})$ are the single-particle wavefunctions, solutions of equations (8.17)–(8.20).

The quantity $\beta_{\lambda\alpha}$ is associated with the deformation parameters introduced in equation (8.22). In particular, for $\lambda = 2$ and $\mu = 0$, we have $\alpha_{20} = \beta_2/\sqrt{5}$. A similar matrix element can be obtained when the fermion, instead of a particle above the Fermi surface, is a hole in the Fermi sea (see Appendix A, equations (A.47), (A.48), for a discussion of the relation between the corresponding matrix element and the matrix element (8.31)). Aside from these matrix elements, the particle-vibration coupling Hamiltonian allows for two other matrix elements (see Fig. 8.11)

$$\langle \alpha | \delta U | \nu_k(\nu_i)^{-1} \rangle = \Lambda_\alpha \langle \tilde{\nu}_i | \hat{F} | \nu_k \rangle, \tag{8.34}$$

and

$$\langle \alpha \nu_k(\nu_i)^{-1} | \delta U | 0 \rangle = \Lambda_\alpha \langle \tilde{\nu}_i | \hat{F} | \nu_k \rangle^*, \tag{8.35}$$

where the symbol $|\nu_i^{-1}\rangle$ denotes a hole state while $|\tilde{\nu}_i\rangle$ is the state time-reversed to the state $|\nu_i\rangle$ (equation (A.41)). The first matrix element corresponds to the process in which a particle falls into a hole giving its energy and angular momentum to a vibrational state $|\alpha\rangle$. The matrix element (8.35) is associated with the process by which the vacuum becomes virtually excited through the simultaneous presence of a particle, a hole and a vibration.

8.3.1 RPA dispersion relation

Equation (8.28) for δU describes the coupling of single-particle motion to a vibrational mode with collective coordinate α. In the random phase approximation (RPA) a collective vibration can be viewed as a correlated particle–hole excitation, which, in the independent particle basis, corresponds to a linear combination of particle–hole excitations. A separable version of the RPA can be derived by recognizing the dual character of equation (8.28) for δU in the sense that the collective mode can be excited through the field $\hat{\alpha}$ as well as through the field $\hat{F}$ (see Fig. 8.12 and Appendix C, Section C.2). More explicitly we impose
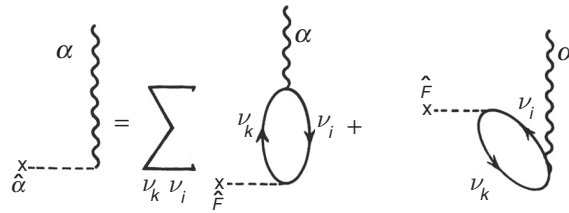
Figure 8.12. Excitation of the collective vibration in terms of the operators $\hat{\alpha}$ and $\hat{F}$. After Bohr and Mottelson (1975).

a self-consistency condition that the transition amplitude,

$$\langle \alpha | \hat{\alpha} | 0 \rangle = \sqrt{\frac{\hbar \omega_\alpha}{2C_\alpha}}, \tag{8.36}$$

should be equal to (see Fig. 8.12)

$$\langle \alpha | \hat{F} | 0 \rangle = \sum_{\nu_k, \nu_i} \left\{ \frac{\langle \alpha | \delta U | \nu_k \nu_i^{-1} \rangle \langle \nu_k \nu_i^{-1} | \hat{F} | 0 \rangle}{\hbar \omega_\alpha - (\varepsilon_{\nu_k} - \varepsilon_{\nu_i})} \right.$$
$$\left. + \frac{\langle \alpha | \hat{F} | \nu_k \nu_i^{-1}; \alpha \rangle \langle \nu_k \nu_i^{-1}; \alpha | \delta U | 0 \rangle}{-(\hbar \omega_\alpha + (\varepsilon_{\nu_k} - \varepsilon_{\nu_i}))} \right\}. \tag{8.37}$$

This expression for the transition matrix element can be expressed in terms of RPA amplitudes as

$$\langle \alpha | \hat{F} | 0 \rangle = - \sum_{\nu_k, \nu_i} (X_\alpha(\nu_k \nu_i) + Y_\alpha(\nu_k \nu_i)) \langle \tilde{\nu}_i | \hat{F} | \nu_k \rangle,$$

where

$$\left. \begin{array}{c} X_\alpha(\nu_k \nu_i) \\ Y_\alpha(\nu_k \nu_i) \end{array} \right\} = \pm \frac{\Lambda_\alpha \langle \tilde{\nu}_i | \hat{F} | \nu_k \rangle}{(\varepsilon_{\nu_k} - \varepsilon_{\nu_i}) \mp \hbar \omega_\alpha}. \tag{8.38}$$

For simplicity, the matrix element $\langle \tilde{\nu}_i | \hat{F} | \nu_k \rangle$ has been assumed to be real. Equating the relations given in equations (8.36) and (8.37) one obtains the RPA dispersion relation

$$W(\hbar \omega_\alpha) = \sum_{\nu_k, \nu_i} \frac{2(\varepsilon_{\nu_k} - \varepsilon_{\nu_i}) |\langle \tilde{\nu}_i | \hat{F} | \nu_k \rangle|^2}{(\varepsilon_{\nu_k} - \varepsilon_{\nu_i})^2 - (\hbar \omega_\alpha)^2} = \frac{1}{\kappa}. \tag{8.39}$$

Equation (8.39) can be solved numerically for values of $\hbar \omega_\alpha$ as illustrated in Fig. 8.13.
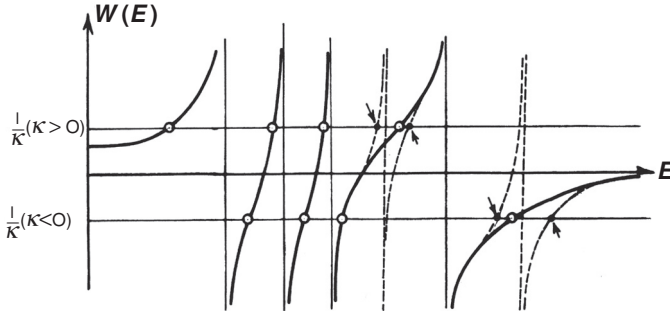
Figure 8.13. Graphical solution of the RPA dispersion relation, equation (8.39).

In keeping with the relation given in equation (8.37) one can write the phonon creation operator as

$$\Gamma_\alpha^\dagger = \sum_{v_k, v_i} X_\alpha(v_k, v_i)\Gamma_{v_k v_i}^\dagger + Y_\alpha(v_k, v_i)\Gamma_{v_k v_i},\qquad(8.40)$$

where $\Gamma_{v_k v_i}^\dagger = a_{v_k}^\dagger a_{v_i}$ and $\Gamma_{v_k v_i} = (a_{v_k}^\dagger a_{v_i})^\dagger$ are creation and annihilation operators of pairs of fermions which are assumed to display boson commutation relations as $\Gamma_\alpha^\dagger$ and Γ_α do (see Appendix A, Section A.4). This is the essence of the so-called random phase approximation (RPA). Consequently,

$$1 = [\Gamma_\alpha, \Gamma_\alpha^\dagger] = \sum_{v_k, v_i}(X_\alpha^2(v_k, v_i) - Y_\alpha^2(v_k, v_i)),\qquad(8.41)$$

a relation which ensures that the one-phonon state $|\alpha\rangle = \Gamma_\alpha^\dagger|0\rangle_{\mathrm{B}}$ is normalized. Equation (8.41) provides the following microscopic expression for the square of the particle-vibration coupling strength

$$\Lambda_\alpha^2 = \left\{2\hbar\omega_\alpha \sum_{v_k, v_i} \frac{2(\varepsilon_{v_k} - \varepsilon_{v_i})|\langle \tilde{v}_i|\hat{F}|v_k\rangle|^2}{[(\varepsilon_{v_k} - \varepsilon_{v_i})^2 - (\hbar\omega_\alpha)^2]^2}\right\}^{-1}$$
$$= \left(\frac{\partial W(E)}{\partial E}\Big|_{E=\hbar\omega_\alpha}\right)^{-1}.\qquad(8.42)$$

Because $(\Lambda_\alpha/\kappa)^2 = (\hbar\omega_\alpha/2C_\alpha)$, the above relation also provides the value of the transition probability $\langle\alpha|\hat{F}|0\rangle^2$.

Making use of the relation given in equation (8.41) and of the corresponding relations obtained from $[\Gamma_\alpha, \Gamma_\alpha] = [\Gamma_\alpha^\dagger, \Gamma_\alpha^\dagger] = 0$, one can invert the equation (8.40) obtaining

$$\Gamma_{v_k v_i}^\dagger = \sum_\alpha X_\alpha(v_k, v_i)\Gamma_\alpha^\dagger - Y_\alpha(v_k, v_i)\Gamma_\alpha.\qquad(8.43)$$

The dispersion relation (8.39) and the expression (8.42) for the normalization constant Λ_α can also be obtained with a separable interaction

$$\delta U_s = -\kappa \hat{F} \hat{F}^+, \tag{8.44}$$

with

$$\hat{F} = \sum_{\nu_k, \nu_i} \langle \nu_k | F | \nu_i \rangle \Gamma^\dagger_{\nu_k \nu_i} + \langle \tilde{\nu}_i | F | \nu_k \rangle \Gamma_{\nu_k \nu_i}. \tag{8.45}$$

Let us comment on the general features of the graphical solutions of equation (8.39), as schematically displayed in Fig. 8.13. The poles of the dispersion relation $W(E)$ correspond to the values of the particle–hole excitation energies. Each root $\hbar \omega_\alpha$ is, in general, bound by two poles and there are as many states $|\alpha\rangle$ as particle–hole states $|\nu_k \nu_i^{-1}\rangle$. The collectivity of a state $|\alpha\rangle$ is measured by the normalization constant Λ_α^2 given in equation (8.42) which is equal to the inverse of the derivative of the dispersion relation $W(E)$ with respect to E at the value $E = \hbar \omega_\alpha$. Consequently, roots which are bound by two poles with similar energies will display little collectivity, as the associated derivative at the corresponding root is very large. Because of this, a single amplitude $X_\alpha(\nu_k, \nu_i)$ will dominate the microscopic structure of the associated wavefunction (see equations (8.27), (8.38) and (8.40)). Collective modes are possible when there is a gap in the particle–hole excitation spectrum. This can happen either at low excitation energies (≤ 3–4 MeV), in connection with the spin–orbit splitting of single-particle levels in medium-heavy nuclei, or at high excitation energies in connection with the energy separation between major shells.

From equation (8.36) and the RPA self-consistency condition (see Appendix C, equation (C.5)), the transition amplitude is given by the relation

$$\langle \alpha | \hat{F} | 0 \rangle = (\hbar \omega_\alpha / 2 C_\alpha)^{1/2} = \frac{\beta_\alpha}{\sqrt{(2\lambda_\alpha + 1)}}. \tag{8.46}$$

Typical values of β_α associated with these collective states are $\beta_\alpha \approx 0.08$–0.1. The corresponding excitation energies are 1–2 MeV for low-lying surface vibrational states, and 10–15 MeV for high-lying states (giant resonances).

An interesting feature of the spectrum emerging from the dispersion relation given in equation (8.39) is the fact that the nucleus displays collective states with low and high frequencies, compared with the energy difference $\hbar \omega_0 (\approx 41 A^{-1/3}$ MeV) between major shells. The low-frequency modes are intimately connected with deformations (plastic behaviour, Chapter 7). High-frequency giant resonances are, on the other hand, related to the small amplitude oscillations (elastic behaviour, see Section 8.3).

To study giant resonances in nuclei lying along the valley of stability, the independent particle model is quite adequate. For a description of the low part of the spectrum, the independent particle model breaks down completely. One

must at least include the pairing interaction in the dynamics of the system (the same seems to be true in the case of giant resonances in exotic (halo) nuclei, in connection with the so-called 'pygmy' resonances (see, e.g. Frascaria *et al.* (2004)). The corresponding theory is called quasiparticle random phase approximation (QRPA, see Section 3.9 and Appendix J), The QRPA dispersion relation corresponding to equation (8.39) is

$$\sum_{\bar{\nu}\nu'} \frac{2(E_\nu + E_{\nu'})|\langle \nu'\bar{\nu}|\hat{F}|0\rangle|^2}{(E_\nu + E_{\nu'})^2 - (\hbar\omega_\alpha)^2} = \frac{1}{\kappa}, \tag{8.47}$$

where $\langle \nu'\bar{\nu}|\hat{F}|0\rangle$ is the matrix element of the interaction operator between the BCS vacuum state $|0\rangle$ and the two-quasiparticle state $|\nu'\bar{\nu}\rangle$. The solutions of the QRPA dispersion relation associated with the high-lying part of the spectrum (giant resonances) essentially coincide with those of equation (8.39). The low-energy part is, however, strongly modified. This is because for levels ν and ν' lying close to the Fermi energy the matrix element $\langle \nu'\bar{\nu}|\hat{F}|0\rangle$ contains U, V-factors which differ strongly from the independent particle model values of 0 or 1. The two-quasiparticle energy $E_\nu + E_{\nu'}$ depends on the pairing gap and is larger than the particle–hole excitation energy $\varepsilon_{\nu_k} - \varepsilon_{\nu_i}$. For simple estimates one can use the liquid drop model to calculated the restoring force and the pair hopping model to work out the inertia of the system, as already explained in Section 7.3.

8.3.2 Sum rules

The random phase approximation provides a diagonalization of the particle-vibration coupling Hamiltonian within the harmonic approximation. It is then natural that, as stated before, the number of states $|\alpha\rangle$ is equal to the number of particle–hole states $|\nu_k \nu_i^{-1}\rangle$ coupled to the quantum numbers of the vibration which form the basis states. Provided that the interaction among the fermions is velocity independent, the product of the energy of these states and the square of matrix elements between a particle and a hole state of any one-body operator which only depends on the spatial coordinate is a model-independent quantity, reflecting very general properties of the system as a whole. This result is known as an energy weighted sum rule (EWSR). In the case of dipole excitations it is proportional to the total number of charged particles of the system, being also proportional to the photoabsorption cross-section. One of the basic conditions to be fulfilled by any theoretical treatment used to diagonalize the residual interaction between particle–hole states should be to conserve the corresponding sum rule.

The importance of sum rules in the study of vibrational motion is that they are connected to basic operator identities which restrict the possible matrix elements

in a physical system. Also, through the use of sum rules it is possible to assess the collectivity of a given excitation. Furthermore, sum rules provide an upper limit to the energy that can be transferred to a nucleus under the action of an external field (Broglia and Winther (1991)). The subject of sum rules is quite general and in what follows we will only touch upon it. In particular we will discuss sum rules associated with spatially dependent single-particle fields.

It is simple to prove the EWSR in the form

$$\sum_n |\langle 0|\hat{F}|n\rangle|^2(E_n - E_0) = \tfrac{1}{2}\langle 0|[\hat{F}, [H, \hat{F}]]|0\rangle, \tag{8.48}$$

where n labels the complete set of eigenstates of the Hamiltonian H, E_n are the corresponding eigenvalues and $|0\rangle$ is the exact ground-state wavefunction. An extension of the energy weighted sum rule to the RPA was proved by Thouless (1961a). It has the same form as equation (8.48), but the meaning of the terms is different. The operator $\hat{F}$ is restricted to be a single-particle operator and the factors $(E_n - E_0)$ and $\langle 0|\hat{F}|n\rangle$ are RPA excitation energies and transition amplitudes. The matrix element on the right-hand side should be evaluated with the Hartree–Fock self-consistent ground-state wavefunction. There is an analogous generalization to the quasiparticle RPA. The proof of the RPA sum rule (8.48) in Thouless (1961a) holds when the potential V is a sum of two-body density-independent interactions. Problems which arise with density dependent forces have been discussed by Blaizot and Gogny (1977).

The right-hand side of eq.(8.48) can be simplified if $\hat{F} = \Sigma_k F(\vec{r}_k)$ is a one-particle operator, depending only on the spatial coordinates, and the potential energy terms in the Hamiltonian $H = T + V$ are local functions of the coordinates. Then $[V, F] = 0$ and the double commutator has contributions only from the kinetic energy part of the Hamiltonian. The double commutator can be expressed in terms of derivatives of F so that

$$\tfrac{1}{2}\langle 0|[\hat{F}, [H, \hat{F}]]|0\rangle = \tfrac{1}{2}\langle 0|[\hat{F}, [T, \hat{F}]]|0\rangle$$

$$= \langle 0|\sum_k \frac{\hbar^2}{2m}(\vec{\nabla}_k \hat{F}(\vec{r}_k))^2|0\rangle, \tag{8.49}$$

where the last term implies the diagonal matrix element in the ground state. The average in equation (8.49) can be replaced by an integral over the density $\rho(r)$

$$\sum_n |\langle 0|\hat{F}|n\rangle|^2(E_n - E_0) = \frac{\hbar^2}{2m}\int d^3r \,|\vec{\nabla}\hat{F}|^2\varrho(\vec{r}). \tag{8.50}$$

There is an analogous classical result for the reaction of a system in equilibrium to an impulsive field which gives each particle a momentum $\vec{\nabla}\hat{F}$. On average, the particles start at rest so their average energy after the sudden impulse is $\hbar^2|\vec{\nabla}\hat{F}|^2/2m$. This result is consistent with the fact that the energy weighted sum

rule does not depend on the interactions acting among the nucleons, because the energy is absorbed in a very short time. On the other hand the nuclear forces accelerate the nucleons, and a longer time is required to produce a change in their velocities. Equation (8.48) also holds in the RPA provided that the factors on the left-hand side are interpreted as RPA energies and transition amplitudes (see, e.g. Bortignon *et al.* (1998)).

The energy weighted sum rule most often used for finite systems is associated with multipole fields, $F(\vec{r}) = r^L Y_{LM}(\hat{r})$. When the density $\rho(r)$ is spherically symmetrical the integral on the right-hand side of equation (8.50) can be simplified and

$$\sum_n |\langle 0|r^L Y_{LM}|n\rangle|^2 (E_n - E_0) = \frac{\hbar^2}{2m} \frac{(2L+1)L}{4\pi} \int d^3r \, r^{2L-2} \varrho$$

$$= \frac{\hbar^2}{2m} L(2L+1) \frac{A}{4\pi} \langle r^{2L-2}\rangle. \qquad (8.51)$$

8.3.3 Frequency of the giant quadrupole resonance

The mean energy of the giant quadrupole resonance in a spherical nucleus can be calculated from the dispersion relation (8.39). In a self-sustained vibration the changes in the density should be proportional to the changes in the potential. The coupling constant κ in equation (8.28) provides this proportionality factor. As discussed in Section 8.3.1 (see Fig. 8.12) and also in Appendix C, the operators $\hat{\alpha}$ and $\hat{F}$ can be viewed as the collective and the single-particle representation of the same field. In other words, equation (8.28) can also be thought of in terms of a separable two-body residual interaction (see equation (8.44))

$$v(\vec{r}, \vec{r'}) = -\kappa \hat{F}(\vec{r})\hat{F}^+(\vec{r'}). \qquad (8.52)$$

The appropriate choice of $\hat{F}(\vec{r})$ for a quadrupole resonance is the quadrupole field

$$\hat{F}(\vec{r}) \equiv F_{2M}(\vec{r}) = r^2 Y_{2M}(\hat{r}).$$

In the case of an isoscalar giant resonance the coupling constant κ can be estimated by an argument which has two parts (Bertsch and Broglia (1994)). The first is the assumption that the time-dependent displacements associated with this field are those of an irrotational incompressible fluid with a velocity potential $F_{2M}(\vec{r})$

$$\vec{u}(\vec{r}, t) = \alpha(t)\vec{u}_0(\vec{r}),$$

with

$$\vec{u}_0(\vec{r}) = \vec{\nabla} F_{2M}(\vec{r}).$$

The time-dependence of $\vec{u}(\vec{r}, t)$ is carried by the collective coordinate $\alpha(t)$. The incompressibility follows from the relation

$$\vec{\nabla} \cdot \vec{u} = \alpha \nabla^2 F_{2M}(\vec{r}) = 0. \tag{8.53}$$

The second assumption is that the transition potential must be consistent with the change in the single-particle density, i.e. they should be generated by the same velocity field $\vec{u}(\vec{r}, t)$. This requirement is an extension to the dynamical case of the self-consistent relation between mean field and ground-state density in Hartree–Fock theory.

Let us carry out the calculations for a generic field $F_{LM} = r^L Y_{LM}$ and then particularize it for $L = 2$. The transition density and potential associated with the velocity field $\vec{u}$ are

$$\delta\varrho = \varrho(\vec{r} + \vec{u}) - \varrho(\vec{r}) = \alpha(t)\vec{u}_0(\vec{r}) \cdot \vec{\nabla}\varrho = \alpha(t)\vec{\nabla} F_{LM} \cdot \vec{\nabla}\varrho, \tag{8.54}$$

$$\delta\mathcal{U} = \vec{u} \cdot \vec{\nabla}\mathcal{U} = \alpha(t)\vec{\nabla} F_{LM} \cdot m\omega_0^2\vec{r} = \alpha(t)m\omega_0^2 L F_{LM}. \tag{8.55}$$

In this estimate, the harmonic oscillator potential has been used to describe the static field, i.e. $\mathcal{U}(r) = \frac{1}{2}m\omega_0^2 r^2$. The transition potential can also be calculated in terms of the convolution of the transition density and the two-body interaction using equation (8.10),

$$\delta\mathcal{U} = -\kappa_L F_{LM}(\vec{r}) \int d^3r'\, F_{LM}^*(\vec{r'})\delta\varrho. \tag{8.56}$$

Equating the results of equations (8.55) and (8.56) one obtains

$$\kappa_L = -\frac{L\alpha(t)m\omega_0^2}{\int d^3r' F_{LM}^*(\vec{r'})\delta\varrho}. \tag{8.57}$$

The integral in this equation can be simplified using Gauss' theorem and the incompressibility condition equation (8.53)

$$\alpha(t) \int d^3r'\, F_{LM}^* \vec{\nabla} F \cdot \vec{\nabla}\varrho = -\alpha(t) \int d^3r'\, |\nabla F|^2\varrho$$

$$= -L(2L + 1)\alpha(t) \int dr\, r^{2L-2}\varrho$$

$$= -L(2L + 1)\alpha(t)\frac{A}{4\pi}\langle r^{2L-2}\rangle$$

Inserting the result into equation (8.57) the factor $\alpha(t)$ cancels and the coupling parameter κ_L is

$$\kappa_L = \frac{4\pi m\omega_0^2}{(2L + 1)A\langle r^{2L-2}\rangle}. \tag{8.58}$$

For $L = 2$ the coupling parameter is

$$\kappa_2 = \frac{4\pi m\omega_0^2}{5A\langle r^2 \rangle}.$$

Giant quadrupole excitations are produced by promoting particles from an occupied shell with principal quantum number N (harmonic oscillator) to unoccupied shells with principal quantum numbers $N + 2$, $N + 4$, etc. This is because the parity of the single-particle states is $(-1)^N$. Because in the harmonic oscillator the only non-diagonal matrix elements of the field $r^2 Y_{2M}$ are

$$\langle N' | r^2 | N \rangle \propto \delta(N', N \pm 2),$$

the particle–hole excitation energy associated with quadrupole modes is $\varepsilon_{\nu_k} - \varepsilon_{\nu_i} = 2\hbar\omega_0$. The dispersion relation given in equation (8.39) can be written as

$$\frac{\sum_{\nu_k, \nu_i} 2(\varepsilon_{\nu_k} - \varepsilon_{\nu_i}) |\langle \tilde{\nu}_i | r^2 Y_2 | \nu_k \rangle|^2}{(2\hbar\omega_0)^2 - (\hbar\omega_Q)^2} = \frac{1}{\kappa_2}.$$

Making use of the quadrupole energy weighted sum rule (see equation (8.51))

$$\sum_{\nu_k, \nu_i} (\varepsilon_{\nu_k} - \varepsilon_{\nu_i}) |\langle \tilde{\nu}_i | r^2 Y_2 | \nu_k \rangle|^2 = \frac{5}{4\pi} \frac{\hbar^2}{m} A \langle r^2 \rangle, \tag{8.59}$$

the factor $\langle r^2 \rangle$ cancels and one obtains

$$\hbar\omega_Q = \sqrt{(2\hbar\omega_0)^2 - 2(\hbar\omega_0)^2} = \sqrt{2}\hbar\omega_0 = \frac{58}{A^{\frac{1}{3}}} \text{ MeV}. \tag{8.60}$$

In Fig. 8.14 we display the systematics of centroids of the giant quadrupole as a function of mass number. The results are well parametrized by the function

$$\hbar\omega_Q \approx \frac{63}{A^{\frac{1}{3}}} \text{ MeV}, \tag{8.61}$$

which is quite close to the theoretical result given in equation (8.60).

8.3.4 Damping of giant vibrations

One can view giant vibrations as a correlated particle–hole excitation built out of a particle above the Fermi surface and a hole in the Fermi sea. A first estimate of the damping width of giant vibrations can be obtained by assuming that the particle and the hole couple to a more complicated configuration acquiring a width. Then the total width is the sum of individual widths. Because in the damping process we deal with real processes, i.e. processes where the energy is conserved, the energy of the resonance has to be shared between the particle and the hole. The simplest expression one can write for the giant resonance damping
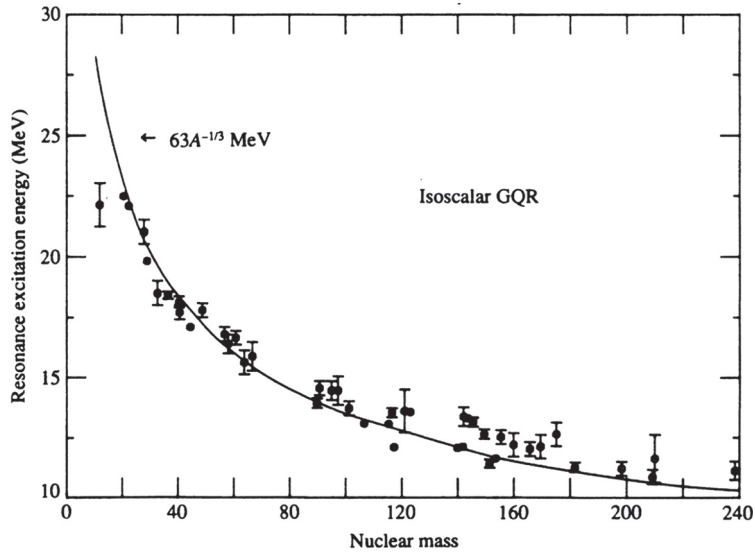
Figure 8.14. Energy systematics of the giant quadrupole resonance (GQR). (from Bertsch and Broglia (1994))

width is then

$$\Gamma^{\downarrow}_{\text{GR}}(\hbar\omega_{\text{GR}}) = \Gamma^{\downarrow}_{p}\left(\frac{\hbar\omega_{\text{GR}}}{2}\right) + \Gamma^{\downarrow}_{h}\left(\frac{\hbar\omega_{\text{GR}}}{2}\right)$$
$$\approx 0.5\hbar\omega_{\text{GR}},$$

(8.62)

where the expressions for $\Gamma^{\downarrow}_{p}$ and $\Gamma^{\downarrow}_{h}$ given in equation (9.15) have been used.

Making use of the expression $\hbar\omega_{Q} \approx 63A^{-1/3}$ MeV, the above equation leads to

$$\Gamma^{\downarrow}_{Q} \approx \frac{30}{A^{\frac{1}{3}}} \text{ MeV}$$

(8.63)

for the damping width of the giant quadrupole resonance. This expression is shown in Fig. 8.15 compared with the experimental findings. The simple estimate overpredicts the experimental findings by roughly 50%.

As will be shown below, the relation given by equation (8.62) neglects important correlation effects between the particle and the hole (Bortignon and Broglia (1981), Bortignon *et al.* (1983), Bertsch *et al.* (1983)). In fact, this relation implies that either the particle or the hole of the correlated particle–hole pair which constitutes a resonance can not only excite a surface vibration, which is true, but also reabsorb the phonon they have excited. This of course is not correct, in that a surface vibration excited by the inelastic scattering of the particles off the nuclear surface can be absorbed at a later time by the hole, and vice versa. In other words, the expression (8.62) takes care only of the (self-energy)
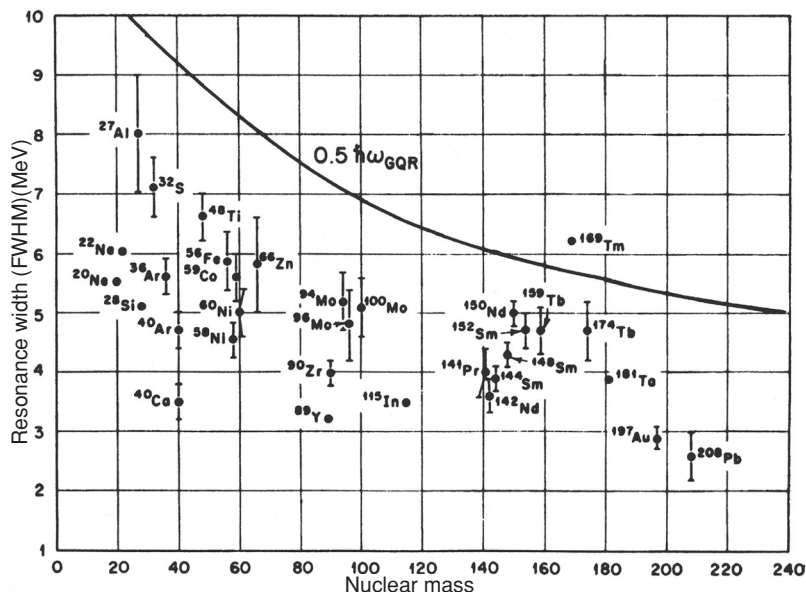
Figure 8.15. Damping width of the giant quadrupole vibration (see Satchler (1977)). The continuous curve corresponds to the estimate given in equation (8.63). Copyright © Società italiana di Fisica.
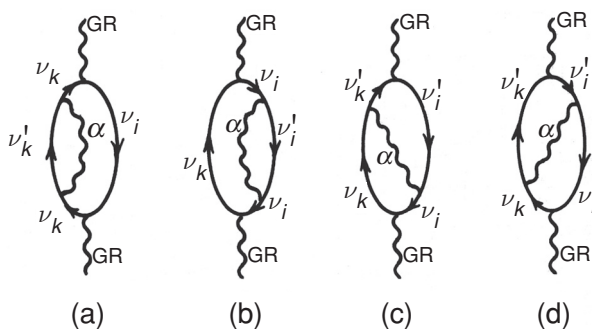

Figure 8.16. Lowest-order processes by which a resonance (GR) couples to a two-particle–two-hole intermediate state (doorway state) containing an uncorrelated particle–hole excitation and a surface vibration.

processes (a) and (b) of Fig. 8.16. We shall see that (vertex correction) processes (c) and (d), where a phonon is exchanged between the fermions, act as a glue between the particle and the hole, preventing, to a large extent, the decay of the resonance, and reducing the contributions (a) and (b) to the damping width. In fact, the self-energy correction to the giant vibration implied by the process of

Fig. 8.16(a) is

$$\Sigma_{\text{self-en}}^{p}(\text{GR}, \omega) = \sum_{v_k, v_i, v_{k'}, \lambda} X_{\text{GR}}^2(v_k, v_i) \frac{V^2(v_k, v_{k'}; \lambda)}{\hbar\omega - ((e_{v_{k'}} - e_{v_i}) + \hbar\omega_\lambda)}$$

$$= \sum_{v_k, v_i} X_{\text{GR}}^2(v_k, v_i)\Sigma(v_k, \omega + e_{v_i}), \tag{8.64}$$

i.e. it is the sum of the contributions of the self-energy of each particle participating in the linear combination of particle–hole excitations describing the resonance. In other words, it is the weighted average of the single-particle self-energies of all the particle–hole configurations. The weighting factor is the probability that the giant vibration will be in a given configuration. The particle self-energies are calculated at an energy $(\hbar\omega + e_{v_i})$, i.e. at an energy lower than the energy of the giant resonance by the amount e_{v_i} $(= \varepsilon_{v_i} - \varepsilon_{\text{F}} < 0)$, which is the energy taken up by the hole of the different particle–hole excitations. A similar expression is obtained for the decay of the hole (see Fig. 8.16(b)), i.e.

$$\Sigma_{\text{self-en}}^{\hbar}(\text{GR}, \omega) = \sum_{v_k, v_i} X_{\text{GR}}^2(v_k, v_i)\Sigma(v_i, \omega - e_{v_k}) \tag{8.65}$$

where now $e_{v_k} = \varepsilon_{v_k} - \varepsilon_{\text{F}} > 0$.

Making the ansatz that (a) the giant resonance is a very correlated state such that one can approximate the amplitudes by $|X| \sim \frac{1}{\sqrt{N}}$, N being the dimension of the particle–hole basis where the RPA solution of the giant vibration has been calculated, and (b) the particle-vibration coupling matrix elements are independent of the configuration, one can write, for both of the expressions given in equations (8.64) and (8.65),

$$\Sigma_{\text{self-en}}^{v}(\text{GR}, \omega) \approx \Sigma(v, \omega - |e_{v'}|), \tag{8.66}$$

where v is either a particle or a hole and v' a hole or a particle respectively. The imaginary part of the above equation leads to the relation (8.62).

The self-energy associated with the process (d) of Fig. 8.16 is

$$\Sigma_{\text{vertex}}(\text{GR}, \omega) = \sum_{v_k, v_i, v_{k'}, v_{i'}} X_{\text{GR}}(v_k v_i) X_{\text{GR}}(v_{k'} v_{i'})$$

$$\times \frac{\langle v_{i'}^{-1}|\hat{F}|v_i^{-1}\rangle \langle v_{k'}|\hat{F}|v_k\rangle^2 \Lambda_\lambda^2}{\hbar\omega - ((e_{v_{k'}} - e_{v_i}) + \hbar\omega_\lambda)}, \tag{8.67}$$

where $|v_i^{-1}\rangle$ represents a state of a hole and $|v_i\rangle$ that of a particle moving in the same single-particle state. The matrix elements between hole states are related to those between particle states according to

$$\langle v_{i'}^{-1}|\hat{F}|v_i^{-1}\rangle = c\langle v_{i'}|\hat{F}|v_i\rangle, \tag{8.68}$$

where c is a phase (i.e. $c^2 = 1$) defined through the relation (see equation (A.49))

$$(\tau \hat{F} \tau^{-1})^\dagger = -c\hat{F}. \tag{8.69}$$

Here τ stands for the time-reversal operator and the dagger identifies Hermitian conjugation. Because an average $\langle \nu_{i'} |F| \nu_i \rangle$ and $\langle \nu_{k'} |F| \nu_k \rangle$ have the same order of magnitude one can approximate the last expression by

$$\Sigma_{\text{vertex}}(\text{GR}, \omega)$$

$$\approx c \sum_{\nu_k, \nu_i, \nu_{k'}} (X_{\text{GR}}(\nu_k \nu_i))^2 \frac{V^2(\nu_{k'}, \nu_k; \lambda)}{\hbar\omega - ((e_{\nu_{k'}} - e_{\nu_i}) + \hbar\omega_\lambda)}. \tag{8.70}$$

A similar expression is obtained for the process depicted in Fig. 8.16(c). Consequently,

$$\frac{\Sigma_{\text{vertex}}}{\Sigma_{\text{self-en}}} \approx c . \tag{8.71}$$

Because the single-particle field $\hat{F}$ is a spin-isospin independent field, $c = -1$. The physical reason for the minus sign in the phase relating processes (a) and (d) of Fig. 8.16 is associated with the fact that the multipole moments of a particle and a hole have different sign, in keeping with the fact that closed-shell systems are spherical.

Under the approximation leading to equation (8.70), there would be a complete cancellation between the different processes contributing to the self-energy operator of the giant resonance, and eventually to its damping width. This result is intimately connected with Furry's theorem of quantum electrodynamics (Furry (1937)), as well as with general arguments on particle conservation (Ward (1950), Takahashi (1957), see also Bortignon *et al.* (1983)). The fact that the subspaces available to the particles (ν_k) and to the holes (ν_i) are different makes the approximations used above not quantitatively accurate although they are qualitatively sound. The cancellation implied by equation (8.71), although conspicuous, is not complete (see also discussion following equation (3.90)).

Numerical calculations indicate that the cancellation discussed above implies a reduction of the contributions stemming from particle- and hole-decay of the order of 30–50%, bringing theory into overall agreement with the experimental findings.

8.4 Correlation energy contribution to nuclear masses

In the present section we discuss some of the consequences that the zero-point fluctuations associated with pairing and surface vibrations have in the nuclear binding energies. Let us start by briefly commenting on the accuracy modern mass formulae have in accounting for the experimental findings.

The best account of the experimental data based on mean-field theory provides a fitting to the 2135 measured masses with N, $Z > 8$ with a r.m.s. (root mean square) error of 0.674 MeV (Goriely *et al.* (2002)). This has been achieved by means of Hartree–Fock–Bardeen–Cooper–Schrieffer (HFBCS) calculations which employ a Skyrme-type zero-range effective force in the mean-field channel, supplemented by a zero-range pairing interaction. The 14-parameter set is named BSk2. As a reference point for the work of Baroni *et al.* (2004) we discuss below, they have considered a parameter set of almost equal quality, denoted by MSk7, where the r.m.s. error is 0.738 MeV (see also Goriely *et al.* (2001)).

Nuclei display both single-particle and collective degrees of freedom. Consequently, the corresponding ground states and associated nuclear masses reflect the effect of the zero-point fluctuations (ZPF) associated with these modes. While mean-field theory includes fluctuations associated with quasiparticles, it is only time-dependent mean-field theory which takes into account the zero-point fluctuations associated with collective vibrations. The need to consider their effect was put forward by Bertsch and Hagino (2001). Realistic calculations for the quadrupole degree of freedom have been performed for light nuclei (Stetcu and Johnson (2002)) and for a few selected isotopes within the so-called generator coordinate method (GCM) (Bender *et al.* (2004)).

Making use of random phase approximation (RPA) Baroni *et al.* (2004) calculated the ground-state correlation energies associated with both surface (quadrupole and octupole modes) and pairing vibrations for the Ca and Pb isotopes. Because pairing vibrations have a collective character only around closed-shell nuclei (being essentially pure two-quasiparticle states lying on top of twice the pairing gap in superfluid systems, see Section 5.2), one expects the associated ZPF (see e.g. Fig. 5.3, (right)) to lead to important corrections to the mass formula of Goriely *et al.* (2002). This is in keeping with the fact that the largest deviations from experiment found in this mass formula are observed in closed-shell systems.

To derive the particle–hole RPA equations, use can be made of the quasi-boson approximation where the RPA ground-state energy is given by (see e.g. Ring and Schuck (1980) see also Sections 6.3 and 6.6)

$$E_{\mathrm{RPA}} = E_{\mathrm{HF}} - (2\lambda + 1) \sum_{\alpha,n} \hbar\omega_\alpha(n) \sum_{ki} \left| Y_{ki}^\alpha(n) \right|^2 , \qquad (8.72)$$

This relation reflects the fact that the amplitudes $Y_{ki}^\alpha(n)$ are directly related to the ground-state correlations induced by the corresponding vibrational modes. The second term of the right-hand side is called the correlation energy.

We now proceed to discuss the expected contributions to the nuclear mass arising from monopole and multipole pairing vibrations in Pb isotopes. Let us start by discussing the monopole pairing-vibration contributions.
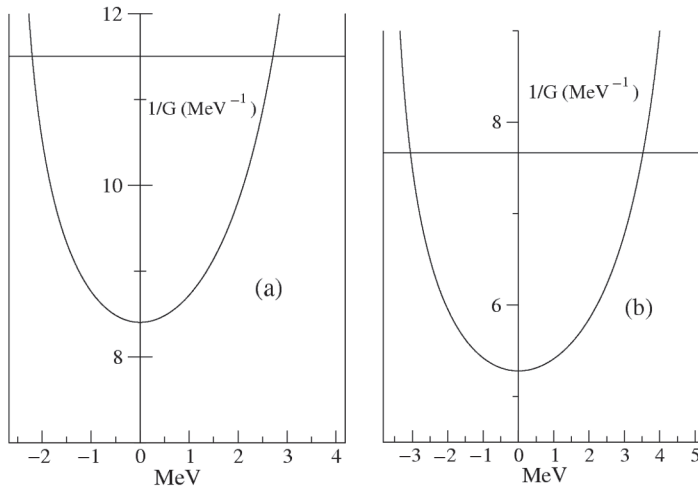
Figure 8.17. Monopole pairing–vibration dispersion relation for (a) neutrons and (b) protons for the nucleus ^{208}Pb. This figure is due to S. Baroni.

Fig. 8.17 shows the dispersion relations given in equation (5.50) calculated for ^{208}Pb for both protons and neutrons (see Section 5.2.1), making use of the valence orbitals of this nucleus. Making use of the fact that the sum of the pairing binding energies of ^{206}Pb and ^{210}Pb (see equations (5.45) and (5.46)) as well as in ^{206}Hg and ^{210}Po are ≈ 2 MeV (in this last case one has to take into account the Coulomb repulsion between the two protons, see e.g. Bortignon *et al.* (1977)), one obtains the values of 2.7 MeV and 2.2 MeV for the neutron pair-addition and pair-removal energies,* the corresponding values for the proton channel being 3.5 MeV and 3.1 MeV respectively. The contributions of the lowest ($n = 1$) pair-addition and pair-subtraction modes have been considered in the calculations because, as a rule, the $n \neq 1$ modes are much less collective.

Inserting the results mentioned above in equation (8.72) and the corresponding Y amplitudes ($= a_1(\omega)$ for ^{208}Pb and $r_1(\omega)$ for ^{206}Pb; see Table 5.1, and equations (6.34)–(6.37)), one obtains the ground-state correlation energy values -0.399 MeV (neutrons) and -0.449 MeV (protons) respectively. Making use of similar quantities associated with pairing vibrations with multipolarity $\lambda \neq 0$ (see Section 5.3.1), in particular quadrupole and hexadecapole pairing vibrations, the corresponding contributions have also been calculated.

In Table 8.1 we show these contributions to the ground-state energy (i.e. E_{RPA} as defined in equation (8.72)) associated with the monopole, quadrupole and

---

* Note that the condition introduced in equation (5.41) (and corresponding to the situation $x = 0.5$ in the two-level model of Fig. 5.1, see Section 5.2) to simplify the discussion of the energy spectrum is here not applicable.

Table 8.1. *Ground-state correlation energies, arising from the neutron* (n) *and proton* (p) *monopole, quadrupole and hexadecapole pairing vibrations in* ^{208}Pb.

0^+		2^+		4^+	
n	p	n	p	n	p
−0.399	−0.449	−0.609	−0.244	−0.189	−0.092

Table 8.2. *Ground-state correlation energies for the* Pb *isotopes.*

	^{204}Pb	^{206}Pb	^{208}Pb	^{210}Pb	^{212}Pb
p–h vibrations	−2.793	−2.709	−2.237	−2.801	−3.173
Pairing vibrations	−0.785	−0.785	−1.981	−0.785	−0.785

hexadecapole pair-addition and pair-removal modes for both neutrons and protons associated with ^{208}Pb, the summed contribution amounting to −1.981 MeV ($\approx$ −1.196 MeV −0.785 MeV).

In Table 8.2 we collect the corresponding contribution for a number of Pb isotopes. As mentioned above, pairing vibrations are collective modes only around closed-shell nuclei, where particles and holes can be clearly distinguished. Consequently (see Chapter 5) we have considered the contribution of neutron pairing vibrations only for the closed-shell system (while the proton pairing vibrations were taken into account for all isotopes). Also shown in Table 8.2 are the contribution to E_{RPA} arising from the low-lying collective particle–hole vibrations calculated by making use of the MSk7 interaction to determine the single-particle states and the particle–hole correlated modes. Quadrupole and octupole vibrations with energy <7 MeV, and exhausting ≥2% of the non-energy weighted sum rule were included in the calculation of E_{RPA}. These conditions essentially select the lowest (one or two) states displaying correlated wavefunctions (see Section 7.3).

Similar calculations were repeated for the calcium isotopes $^{40-48}$Ca. In Table 8.3 the corresponding results are shown, together with the contribution of the particle–hole vibrational modes. When adding the results of Tables 8.2 and 8.3 to the HFBCS MSk7 mass formula of Goriely *et al.* (2001), the parameters of the Skyrme interaction should be refitted in order to provide the best reproduction of experimental masses. This should be done on a large sample of isotopes, a scope which was beyond the purpose of the paper of Baroni *et al.* (2004). If one restricts oneself to Ca isotopes (Pb isotopes) the results in Table 8.4

Table 8.3. *Ground-state correlation energies for the* Ca *isotopes.*

	^{40}Ca	^{42}Ca	^{44}Ca	^{46}Ca	^{48}Ca
p–h vibrations	−0.886	−1.418	−1.606	−1.391	−0.547
pairing vibrations	−4.761	−2.978	−3.239	−3.500	−5.823

Table 8.4. *(first column) Root mean square error associated with the HFBCS MSk7 mass formula of Goriely et al. (2001) and (second column) r.m.s.e. associated with HFBCS MSk7 mass formula (with sligthly adjusted parameters) plus the correlation contributions associated with surface and pairing vibrations calculated in the RPA. The quantity* $\bar{\sigma} = \left(\frac{\sigma_{Ca}^2 + \sigma_{Pb}^2}{2} \right)^{1/2}$ *is shown in the last line.*

	σ (MeV)	
Pb	0.646	0.543
Ca	1.200	0.466
$\bar{\sigma}$	0.964	0.505

are obtained. Averaging the r.m.s. deviations associated with Ca and Pb isotopes leads to a value of 0.505 MeV compared with the value of 0.964 MeV obtained by making use of the results of Goriely *et al.* (2002). Although a global readjustment of the mean-field parameters should be envisaged, the fact that the locally extracted r.m.s. deviations have been reduced by a factor of approximately 2 can be considered meaningful, highlighting the important role that pairing vibrations play in the ground-state nuclear energies.